ACS APPLIED MATERIALS & INTERFACES

www.acsami.org

Research Article

Guest-Induced Phase Switching in a Square Lattice Coordination Network to Enable Selective Adsorption of *p*-Xylene

Shi-Qiang Wang,* Catiúcia R. M. O. Matos, Shaza Darwish, Volodymyr Bon, Yifei Luo, Jun Zhu, Xiaofei Zhang, Zhengtao Xu, Stefan Kaskel, and Michael J. Zaworotko*

Cite This: https://doi.org/10.1021/acsami.5c07908

Read Online

ACCESS | Metrics & More | Article Recommendations | Supporting Information

ABSTRACT: Flexible coordination networks (CNs) offer the potential for exceptional selectivity to enable hydrocarbon separations. The key to performance in such sorbents is guest-induced structural transformations that result in induced-fit binding. Unfortunately, the underlying mechanisms of such transformations remain largely unexplored. Herein, we report an investigation of the phase switching behavior of the square lattice (**sql**) CN $[Cu(4,4'\text{-bipyridine})_2(CF_3CO_2)_2]_n$ (**sql-1-Cu-CF_3CO_2**) induced by xylene adsorption. Competitive adsorption studies in binary and ternary xylene mixtures revealed high *p*-xylene (PX) selectivity of 10.83 over *o*-xylene (OX) and of 14.18 over *m*-xylene (MX), with an overall PX selectivity of 10.01, surpassing most commercial sorbents such as zeolites. Crystallographic studies revealed three distinct xylene-loaded phases with varying pore/channel dimensions and porosity: 1D (void: 33.9%) for PX, 2D (void: 45.8%) for OX, and 3D (void: 48.4%) for MX. The PX-loaded structure exhibited the smallest void but the strongest host−guest interactions, making it the preferred phase for PX separation from xylene mixtures.

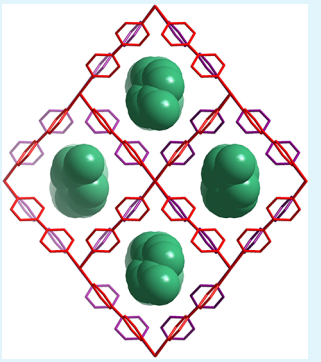

KEYWORDS: *xylene separation, induced-fit, stimuli-responsive material, 2D coordination network, flexible metal−organic material*

Downloaded via Shiqiang Wang on June 27, 2025 at 06:36:26 (UTC).
See https://pubs.acs.org/sharingguidelines for options on how to legitimately share published articles.

INTRODUCTION

The separation and purification of chemical mixtures using traditional methods such as distillation and crystallization account for 10−15% of global energy consumption.[1] With the rising demand for commodity chemicals, there is an urgent need for more energy-efficient purification technologies. One of the most challenging hydrocarbon separations involves the xylene isomers: *o*-xylene (OX), *m*-xylene (MX), and *p*-xylene (PX), which are used to produce fibers, plastics, and fuel additives.[1−3] Among them, PX dominates the xylene market (∼90%) due to its utility for polyethylene terephthalate production.[4] However, the similar physicochemical properties of the xylene isomers render their separation via conventional purification methods energy-intensive and inefficient.[1−4] While adsorption-based technologies have been established for xylene separation, their widespread implementation is hindered by the moderate capacity (∼15 wt %) and selectivity (∼5) of currently used adsorbents, i.e., FAU zeolites.[5]

To address this matter, sorbent materials of many types have been investigated, including molecular materials, such as coordination complexes,[6−9] organic molecules and cages,[10−13] and network materials like porous coordination polymers/networks (PCPs/PCNs) and metal−organic frameworks (MOFs).[14−32] The latter represents a promising class of metal−organic materials (MOMs)[33,34] as they can offering precise control over pore size, shape, and chemistry through crystal engineering or reticular chemistry.[35,36] That there is significant potential for benchmark hydrocarbon separation performance is now evident.[37−42] To date, a considerable number of rigid MOMs with fixed pore geometries have been investigated for xylene separation.[41,42] However, they typically lack the desired combination of strong selectivity (>5) and high adsorption capacity (>15 wt %). In contrast, flexible MOMs are attractive because they can undergo guest-induced structural transformations enabled by breathing, switching/gate-opening, swelling, or induced-fit mechanisms.[43−49] Such sorbent materials can dynamically adjust pore size and shape to enhance adsorption capacity and/or selectivity. Nevertheless, flexible MOMs still remain underexplored, partly due to the difficulty in determining their guest-loaded structures,[50,51] which in turn hampers the elucidation of their structural transformations and, consequently, insight into adsorption mechanisms and structure−property relationships.

Recently, we reported the sorption properties of a family of square lattice (**sql**) coordination networks (CNs) [M-$(bpy)_2(NCS)_2$], **sql-1-M-NCS** (1 = bpy = 4,4′-bipyridine, M = Fe, Co, and Ni).[52−57] The sorption isotherms for gases (CO_2, C_2H_x and C_3H_x) and vapors (xylene isomers) exhibited stepped or sigmoidal profiles (denoted as type F−IV

Received: April 20, 2025
Revised: June 24, 2025
Accepted: June 24, 2025

© XXXX American Chemical Society

isotherms).[48] Crystallographic studies elucidated that the interlayer distance in the closed phase (4.5 Å) can undergo guest-induced expansion to 5.4, 6.3 or 9.1−9.3 Å for the CO_2, C_2H_4 and xylene-loaded phases, respectively.[52−54,57] Such sorbate-dependent phase switching behavior prompted us to evaluate the xylene separation performance of **sql-1-Co-NCS**, which exhibited a strong preference for OX with high adsorption uptake of up to 87.5 wt %.[53] Subsequently, by substituting half of the bpy linkers with 4,4′-bis(4-pyridyl)-tetrazine (bptz), we synthesized a new rectangular mixed-linker **sql** CN $[Co(bpy)(bptz)(NCS)_2]_n$, which exhibited good xylene adsorption capacity (~37 wt %) and high selectivity (~10) for each xylene isomer over ethylbenzene.[58]

In this contribution, we study a new analog of **sql-1-Co-NCS** by substituting the metal cation Co(II) with Cu(II) and replacing the NCS^- counteranion with $CF_3CO_2^-$. This material, **sql-1-Cu-CF_3CO_2**, was investigated for its xylene separation performance through competitive adsorption experiments in binary and ternary liquid xylene mixtures, as analyzed by gas chromatography (GC). Additionally, powder and single-crystal X-ray diffraction (PXRD/SCXRD) studies were conducted to identify the xylene-loaded phases and gain insights into the structural flexibility driven by the host−guest interactions.

RESULTS AND DISCUSSION

Single crystals of $\{[Cu(bpy)_2(CF_3CO_2)_2]\cdot 2TFT\}_n$ (**sql-1-Cu-CF_3CO_2·2TFT**, TFT = α,α,α-trifluorotoluene) were synthesized via solvent diffusion following a procedure similar to that used for **sql-1-Co-NCS·2TFT**.[52] Bulk phase purity was confirmed by PXRD (Figure S1). SCXRD analysis (Table S1) revealed that **sql-1-Cu-CF_3CO_2·2TFT** crystallizes in the monoclinic space group *C2/c* (*a*: 22.59 Å, *b*: 11.16 Å, *c*: 16.43 Å, *β*: 112.54°) and exhibits the expected **sql** topology, with 4-connected Cu(II) cations equatorially coordinated by four bpy ligands and axially by two terminal CF_3CO_2 ligands. TFT molecules reside in the interlayer space with an interlayer distance of 7.7 Å (Figure 1), much larger than that of **sql-1-Co-NCS·2TFT** (6.6 Å), thanks to the bulkier CF_3CO_2 ligands and the more vertical orientation of TFT molecules (Figure S2a,b). The bpy ligands in **sql-1-Cu-CF_3CO_2·2TFT** adopt two conformations: half coplanar and half twisted (43.5°), closely resembling those in **sql-1-Co-NCS·2TFT** (Figure S2c,d).[52] The activated phase, **sql-1-Cu-CF_3CO_2**, was isolated by heating **sql-1-Cu-CF_3CO_2·2TFT** at 100 °C for 30 min as confirmed by thermogravimetric analysis (TGA) and variable-temperature PXRD (Figures 1 and S3−S5). Although crystal structural determination was unsuccessful, the 77 K N_2 and 273 K CO_2 adsorption isotherms indicate that **sql-1-Cu-CF_3CO_2** remains nearly nonporous, with minimal N_2 and CO_2 uptakes at low pressure (Figure S6).

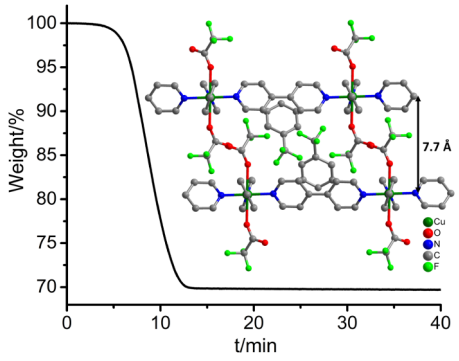

Figure 1. Crystal structure of **sql-1-Cu-CF_3CO_2·2TFT** (H atoms omitted for clarification), which can be fully activated by heating at 100 °C as indicated by the desolvation kinetics curve.

Soaking **sql-1-Cu-CF_3CO_2** in pure OX, MX, and PX resulted in the formation of three distinct phases, as revealed by PXRD (Figure 2a). In contrast, exposure to equimolar binary (PX/MX and PX/OX) or ternary (PX/OX/MX) xylene mixtures led to a single phase with a PXRD pattern that matches the PX-soaked phase (Figure 2a). This suggested to us a strong preference for PX adsorption. To quantify its PX selectivity, adsorbed xylene molecules were extracted using dichloromethane and the compositions were determined by GC (Figure 2b). The GC results show much higher PX peaks, with selectivity values of 10.83 and 14.18 for PX over OX and MX, respectively (Figure S7a,b). The PX selectivity derived from the ternary mixture is 10.01 (Figure S7c), outperforming typical commercial zeolites such as ZSM-5, BaX and KX (Table S2).[5] As seen in Figure 2c,d, these selectivity values are superior or comparable to those of most reported PX-selective adsorbents, including $AgLClO_4$,[7] EtP5/6,[10] AZO-cage,[11] P[4]Q[1]L,[13] MIL-125-NH_2,[16] [Ce(HTCPB)],[17] DUT-8-(Cu),[21] NU-2000,[25] MAF-88,[27] sql-4,5-Zn,[28] polyIRMOF-1−7a,[31] MOF-monoclinic,[59] ZIF-68,[60] Cu(CDC),[61] MIL-140B/MOF-48,[62] CoPzNi,[63] NIIC-30(Ph),[64] HIAM-201,[65] $[Cu_2Cl_4L_2]$,[66] CAU-1/OH,[67] Zn-ETTOB,[68] and MIL-120-(Al),[69] and are surpassed only by a few materials such as Cu-metallocycle,[9] TPBD-αI,[12] MAF-36,[20] ZIF-8/67,[24] Mn-dhbq,[26] MAF-89,[27] HIAM-203,[29] and Co(aip)$(bpy)_{0.5}$.[70]

To understand the high PX selectivity of **sql-1-Cu-CF_3CO_2**, single crystals of the three xylene-loaded phases were prepared using the same solvent diffusion method, with xylene replacing TFT. The corresponding crystal structures were successfully determined (Table S1). Although all the xylene-loaded phases adopt the monoclinic space group *C2/c*, their structural characteristics differ. SCXRD analysis revealed that the OX-loaded phase hosts two OX molecules per unit formula (Figure 3a, denoted as **sql-1-Cu-CF_3CO_2·2OX**), with unit-cell parameters (*a*: 22.47 Å, *b*: 11.15 Å, *c*: 16.46 Å, *β*: 111.75°) and crystal packing (Figure 3d) similar to those of **sql-1-Cu-CF_3CO_2·2TFT**, and the same interlayer distance of 7.7 Å (Figures 1 and 3a). Whereas the MX-loaded phase also accommodates two MX molecules per unit formula (Figure 3b, denoted as **sql-1-Cu-CF_3CO_2·2MX**), its unit-cell parameters (*a*: 15.25 Å, *b*: 16.34 Å, *c*: 16.24 Å, *β*: 106.42°) differ from those of **sql-1-Cu-CF_3CO_2·2OX**, and its interlayer distance (7.8 Å) is slightly larger (Figure 3a,b). Notably, the PX-loaded phase is quite different as it contains only one PX molecule per formula unit (Figure 3c, denoted as **sql-1-Cu-CF_3CO_2·1PX**), with unit-cell parameters (*a*: 14.27 Å, *b*: 14.45 Å, *c*: 16.95 Å, *β*: 106.99°) different from the OX and MX-loaded phases. It also features a reduced interlayer distance (6.8 Å), suggesting a stronger host−host and/or host−guest interactions. In all three xylene-loaded phases, the xylene molecules adopt an ordered and commensurate packing arrangement (Figure 3d-f and S8), occupying exclusively the interlayer space rather than the square grid cavity, as observed in **sql-1-Co-NCS**.[53] The saturation xylene uptakes of **sql-1-Cu-CF_3CO_2** are 35.2 wt % for OX/MX and 17.6 wt % for PX, comparable to most reported PX-selective adsorbents (Figure 2c,d and Table S2).

https://doi.org/10.1021/acsami.5c07908
ACS Appl. Mater. Interfaces XXXX, XXX, XXX−XXX

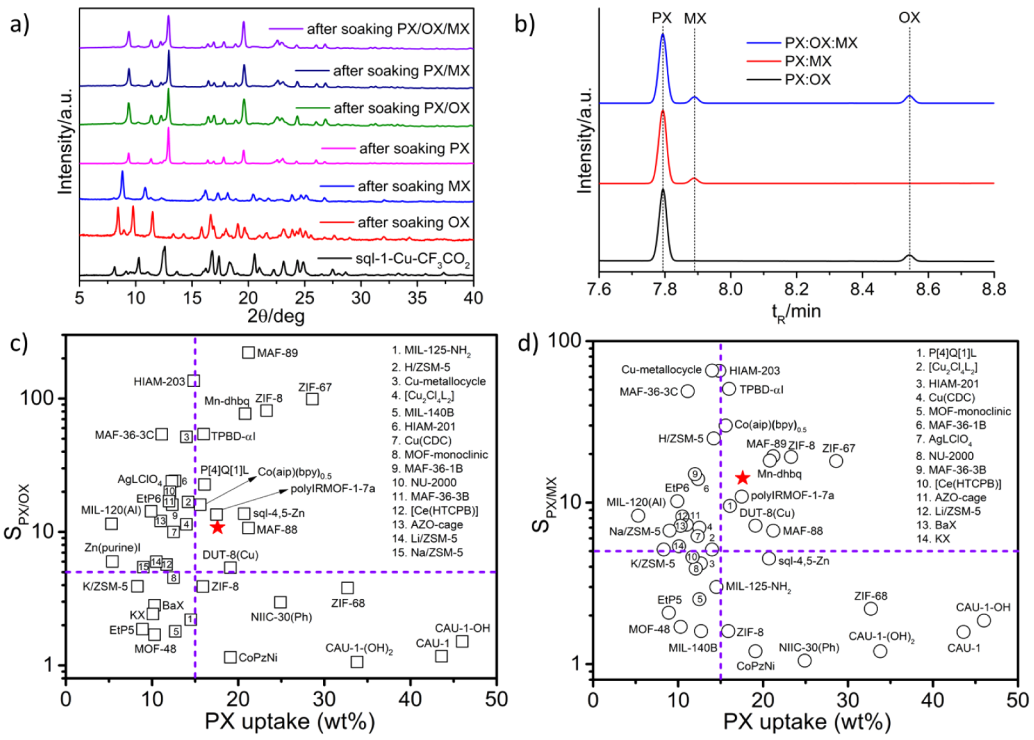

Figure 2. (a) PXRD patterns of **sql-1-Cu-CF_3CO_2** before and after soaking in unary, binary, and ternary xylene solutions. (b) GC analysis of the xylene composition extracted from the soaked samples in the binary and ternary xylene mixtures. (c, d) Comparison of PX selectivity and uptake with PX-selective adsorbents (red star represents for **sql-1-Cu-CF_3CO_2**).

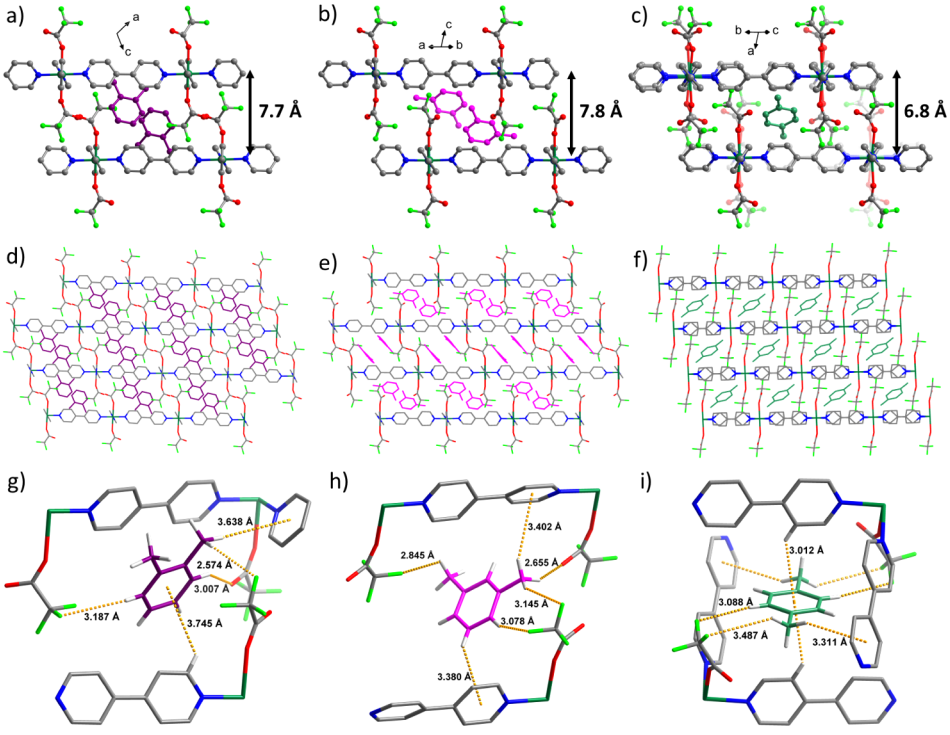

Figure 3. (a–c) Crystal structures, (d–f) packing arrangements, and (g–i) host–guest interactions of **sql-1-Cu-CF_3CO_2·2OX**, **sql-1-Cu-CF_3CO_2·2MX**, and **sql-1-Cu-CF_3CO_2·1PX**, respectively (OX: violet, MX: pink, and PX: sea green).

These different crystal packing patterns resulted in distinct host–guest interactions (Table S3). In the OX-loaded phase (Figure 3g), two types of C–H···π interactions are present: one between the pyridine hydrogen and the benzene ring of OX (3.745 Å), and another between the methyl hydrogen of OX and the pyridine ring (3.638 Å). Additionally, there are two C–H···F and one C–H···O hydrogen bonds. Two H atoms from the phenyl and methyl groups form two C–H···F hydrogen bonds (3.187 and 2.574 Å) with the F atoms of two CF_3CO_2 groups, while another phenyl H atom forms one C–

https://doi.org/10.1021/acsami.5c07908
ACS Appl. Mater. Interfaces XXXX, XXX, XXX–XXX

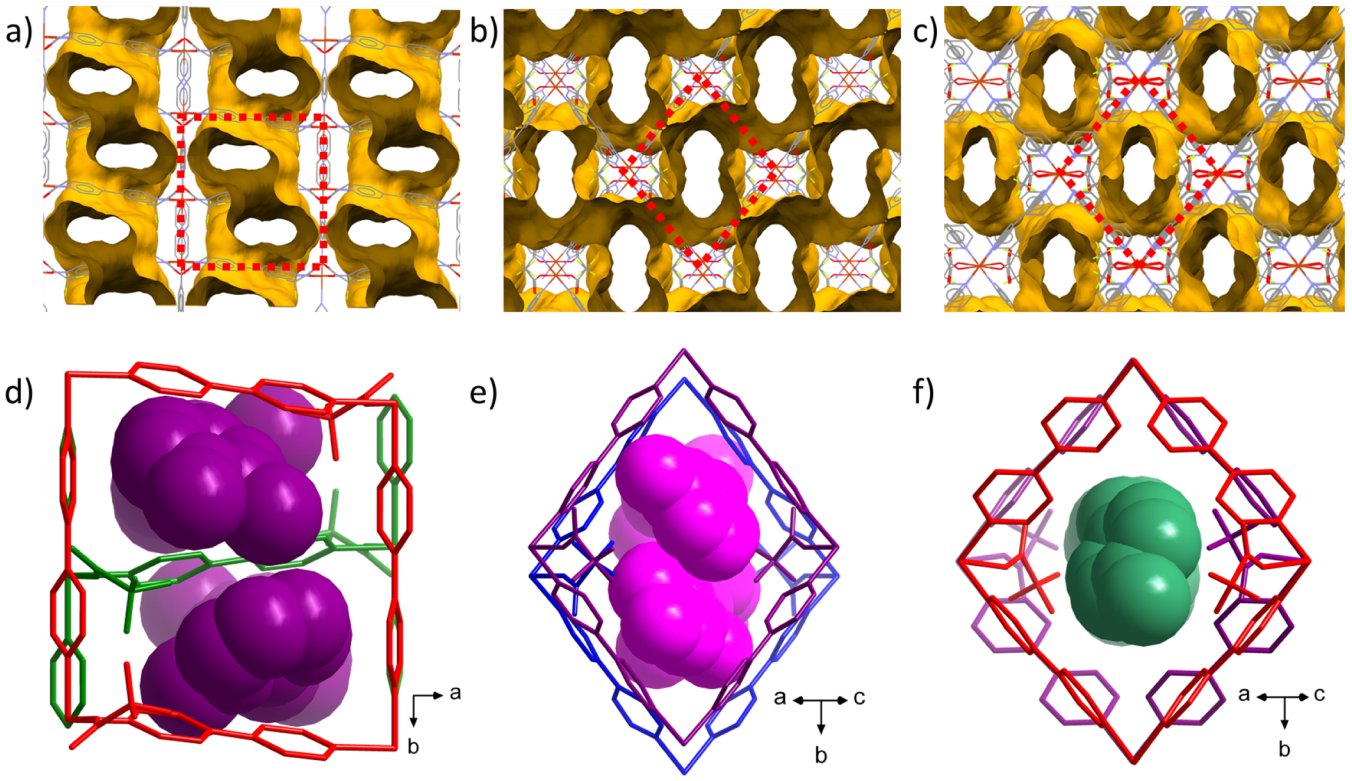

Figure 4. Channel profiles (a–c) and the corresponding enlarged view (d–f) of the red dash line regions for **sql-1-Cu-CF_3CO_2·2OX**, **sql-1-Cu-CF_3CO_2·2MX**, and **sql-1-Cu-CF_3CO_2·1PX**, respectively.

H···O hydrogen bond (3.007 Å) with the O atom of the CF_3CO_2 group. Similarly, in the MX-loaded phase (Figure 3h), three C–H···F and one C–H···O hydrogen bonds are observed. A phenyl H atom and two methyl H atoms of the MX contribute to three C–H···F hydrogen bonds (2.845, 3.078, and 3.145 Å), and another methyl H atom forms one C–H···O hydrogen bond (2.655 Å) with the O atom of the CF_3CO_2 group. One phenyl H and one methyl H atom engage in two C–H···π interactions (3.380 and 3.402 Å) with two pyridine rings. Interestingly, in the PX-loaded phase (Figure 3i), PX establishes symmetric host–guest interactions with the host network. Two methyl H atoms and two phenyl H atoms participate in four symmetric C–H···F hydrogen bonds (3.088 and 3.487 Å). Two additional methyl H atoms form two C–H···π interactions (3.311 Å) with pyridine rings. Furthermore, two H atoms from the pyridine rings contribute to additional C–H···π interactions (3.012 Å) with the phenyl ring of PX. These synergistical noncovalent interactions anchor PX molecules within the pores, explaining why PX is the most strongly adsorbed guest in **sql-1-Cu-CF_3CO_2**. This is further supported by Monte Carlo molecular simulations, which yielded average isosteric heats of xylene adsorption of 132.67, 137.24, and 141.29 kJ mol^{-1} for OX, MX, and PX, respectively.

Due to the adaptive structural rearrangements of the host network induced by xylene isomers, the channel voids (probe radius 1.2 Å) of the MX, OX, and PX-loaded phases are 48.4, 45.8, and 33.9% (Figure 4a–c), respectively. Their channel dimensions also vary (Figures S9–S11): 3D for the MX-loaded phase, 2D for the OX-loaded phase, and 1D for the PX-loaded phase. The 2D channel of **sql-1-Cu-CF_3CO_2·2OX** is divided into two equal segments due to the staggered packing of the adjacent layers (Figure 4d), which merge into one at the connection zone where the OX molecules reside (Figure S9). For the 3D channel of **sql-1-Cu-CF_3CO_2·2MX**, it can be classified as 1D because the channel windows from the other two sides are relatively small (Figure S10). Indeed, when the probe radius is increased to 2.0 Å, these two small windows disappear, and the channel becomes effectively like **sql-1-Cu-CF_3CO_2·1PX** (Figure S11). The main differences between the channels of MX and PX-loaded phases lie in the orientations of the bpy and CF_3CO_2 ligands. In **sql-1-Cu-CF_3CO_2·2MX**, the pyridine rings of the bpy ligands align parallel to the 1D channel while they penetrate into the 1D channel in **sql-1-Cu-CF_3CO_2·1PX** to reduce the channel void. Furthermore, the CF_3CO_2 ligands protrude into the channel from two opposite sides that further constrict the void, thereby allowing only one PX molecule to be accommodated per unit formula. The smallest void in the PX-loaded structure suggests that it requires the least energy input for the structural rearrangement, therefore making **sql-1-Cu-CF_3CO_2·1PX** the preferred phase for xylene mixture adsorption.

Although it is not uncommon that flexible MOMs exhibit varying saturation uptakes for adsorbates with different sizes, the pore or channel dimensions of the guest-loaded phases typically remain unchanged, as exemplified by the MIL-53 family.[15] In contrast, the xylene-induced structural changes in **sql-1-Cu-CF_3CO_2** are unusual, leading to different unit-cell parameters and host–guest ratios (1:1 for PX and 1:2 for OX/MX), along with three distinct pore/channel dimensions ranging from 1D to 3D. This behavior also differs from that of **sql-1-Co-NCS**,[53] where the host–guest ratio remains 1:4 for all three xylene isomers, despite variations in unit-cell parameters. These differences arise from the flexibility imparted by the clay-like nature of the 2D layered structure, which is held by noncovalent interactions. This enables both

https://doi.org/10.1021/acsami.5c07908
ACS Appl. Mater. Interfaces XXXX, XXX, XXX–XXX

phase switching/gate-opening (global structural transitions such as layer expansion and sliding) and induced-fit behavior (local structural adaptations such as ligand rotation and network grid deformation), as summarized in Table S4. In addition, **sql-1-Co-NCS** exhibits OX selectivity, whereas **sql-1-Cu-CF_3CO_2** is PX-selective, further demonstrating how the pore size, shape, and chemistry profoundly impact guest binding, and consequently, uptake and selectivity. These findings highlight the versatility of 2D switching coordination networks in hydrocarbon separations.

CONCLUSIONS

In conclusion, we report herein an investigation of the xylene-induced phase-switching behavior of **sql-1-Cu-CF_3CO_2** through xylene adsorption studies under equilibrium conditions. Its dynamic separation performance, which is relevant to industrial simulated moving bed processes, deserves further investigation through breakthrough experiments. Based on several previous examples,[14,15] it is expected to exhibit selectivity trends similar to those observed in equilibrium mixture adsorption experiments. While flexible MOMs have been investigated for their guest-induced structural changes, the emergence of distinct pore profiles in 2D switching CNs induced by xylene isomers remains rare. Crystallographic studies revealed that the choice of metal center and counteranion strongly influences the selective preference of flexible MOMs. Combined with PX selectivity exceeding 10 and PX uptake of 17.6%, **sql-1-Cu-CF_3CO_2** demonstrates promising separation performance compared to zeolites and other types of adsorbents. To our knowledge, this is only the second example of a 2D MOM exhibiting PX selectivity, following **sql-4,5-Zn**.[28] However, there is still room for improvement in xylene uptake, as **sql-1-Co-NCS** adsorbs >85 wt % of xylenes.[53] In addition, its limited thermal stability (~140 °C) may hinder recyclability (Figure S12) and underscores the need to develop more thermally robust materials. Further investigations will focus on exploring the adsorption behavior of other aromatic hydrocarbons in this family of 2D switching layered materials.

EXPERIMENTAL SECTION

All materials were used as received from commercial sources.

Synthesis of Square Lattice (sql) Coordination Networks (CNs). $\{[Cu(bpy)_2(CF_3CO_2)_2]\cdot 2TFT\}_n$ (**sql-1-Cu-CF_3CO_2·2TFT**) was prepared by the solvent diffusion method. In a typical procedure, a mixture of 2.5 mL methanol and 2.5 mL α,α,α-trifluorotoluene (TFT) was slowly layered over 4,4′-bipyridine (0.3 mmol, 46.8 mg) dissolved in 5 mL TFT. A solution of $Cu(CF_3CO_2)_2$ (0.15 mmol, 43.5 mg) in 5 mL methanol was carefully layered over the methanol/TFT layer. The solution was left undisturbed for a few days to yield turquoise block crystals, which were collected by filtration and washed with TFT three times.

$\{[Cu(bpy)_2(CF_3CO_2)_2]\cdot 2OX\}_n$ (**sql-1-Cu-CF_3CO_2·2OX**), $\{[Cu(bpy)_2(CF_3CO_2)_2]\cdot 2MX\}_n$ (**sql-1-Cu-CF_3CO_2·2MX**), and $\{[Cu(bpy)_2(CF_3CO_2)_2]\cdot 1PX\}_n$ (**sql-1-Cu-CF_3CO_2·1PX**) were prepared using the same method, with TFT replaced by OX, MX, and PX as the solvent media, respectively.

Single-Crystal X-Ray Diffraction Measurements. Suitable single crystals of all compounds were chosen for single crystal X-ray diffraction measurements. The data was collected on a Bruker D8 Quest diffractometer equipped with a IμS microfocus Cu anode (λ = 1.54178 Å) and Photon II detector. For low temperature measurements, an open-flow nitrogen attachment from Oxford Cryosystem was used. In all cases, data was indexed, integrated and scaled in APEX3. Absorption correction was performed by multiscan method. Space groups were determined using XPREP implemented in APEX3. Structures were solved using an intrinsic phasing method (SHELXT) and refined on F^2 using nonlinear least-squares techniques with SHELXL contained in OLEX2 v1.2.8 programs packages. All non-hydrogen atoms were refined anisotropically. Hydrogen atoms were located from the molecular geometry at idealized positions and assigned isotropic thermal parameters depending on the equivalent displacement parameters of their carriers.

Crystallographic data for the as-synthesized **sql** CNs are summarized in Table S1. All crystal structures (open phases) have been deposited with the Cambridge Crystallographic Data Centre (CCDC 2433537−2433540).

Thermogravimetric Analysis (TGA). TGA experiments were conducted under N_2 atmosphere using a TA Instruments Q50 thermal analyzer between room temperature (rt) and 500 °C at a constant rate of 10 °C/min. Desolvation kinetics were measured using a ramp-hold program, where the temperature was raised from rt at 10 °C/min and held at 100 °C for 30 min.

Powder X-Ray Diffraction. Powder X-ray diffraction experiments were conducted using microcrystalline samples on a Panalytical Empyrean diffractometer (40 kV, 40 mA, Cu K$\alpha_{1,2}$, λ = 1.5418 Å). A scan speed of 0.111747°/s (6.7°/min), with a step size of 0.026° in 2θ was used at room temperature with a range of 5°< 2θ < 40°.

Variable Temperature Powder X-Ray Diffraction. For VT-PXRD experiments, reflections were collected on Philips X'Pert diffractometer (40 kV, 40 mA, Cu K$\alpha_{1,2}$, λ = 1.5418 Å) at 10 °C intervals from 25 to 120 °C by heating at 1 °C/min under N_2 atmosphere. Water cooling system was adopted to control the temperature. Diffraction patterns were collected in the 2θ range of 5−40°.

Gas Adsorption. N_2 and CO_2 adsorption experiments of **sql-1-Cu-CF_3CO_2** were conducted on the Micromeritics TriStar II PLUS 3030 at 77 and 273 K, respectively. The measurement temperatures were maintained using a 4 L Dewar flask filled with liquid nitrogen (for 77 K) or a Julabo F25-ME chiller (for 273 K).

Xylene Selectivity Studies. About 20 mg samples of **sql-1-Cu-CF_3CO_2** were separately immersed in 3 mL equimolar binary or ternary liquid of xylene isomers for 2 days to ensure saturation uptake. The saturated samples were then filtered and air-dried (ca. 15 min) under ambient conditions (*ca.* 20 °C) to remove xylenes adhering to the surface of samples. After that, the samples were soaked in 3 mL dichloromethane (DCM) for 2 days. The supernatant of each sample was collected for gas chromatography (GC) measurement. The typical procedure was reported in our recent publication,[12] where GC traces of pure xylene isomers were recorded and subsequently used as references in this study. GC analyses were carried out on an Agilent 6890A gas chromatograph fitted with a 7683B ALS (automated liquid sampler) equipped with a flame ionization detector (FID). The column used was an Agilent DBWax column (length: 30 m, inner diameter: 320 μm, film thickness: 0.25 μm). The injector and detector were kept at 220 °C and nitrogen was used as carrier gas with a flow rate of 1 mL/min. One μL of each liquid sample was injected through the GC inlet with a split ratio of 100:1 and a split flow

https://doi.org/10.1021/acsami.5c07908
ACS Appl. Mater. Interfaces XXXX, XXX, XXX−XXX

rate of 142.45 mL/min. Dichloromethane HPLC/GC grade 99.9% (Sigma-Aldrich) was used as the eluent and solvent.

Molecular Simulations. Molecular simulations were conducted based on the crystal structures of xylene-loaded phases in the *P1* space group, with xylene molecules in the pores removed prior to simulation. Xylene sorption at 298 K and 1 kPa was performed using the Sorption module in Materials Studio (task: fixed pressure; quality: ultrafine; equilibration steps: 1,000,000; Monte Carlo method: Metropolis; force field: Universal). The isosteric heats of adsorption for each xylene isomer were obtained as output.

■ ASSOCIATED CONTENT

Supporting Information

The Supporting Information is available free of charge at https://pubs.acs.org/doi/10.1021/acsami.5c07908.

TGA curve, PXRD pattern, N_2 adsorption isotherm, etc. (PDF)

Crystal structural file of **sql-1-Cu-CF_3CO_2·2TFT** (CIF)

Crystal structural file of **sql-1-Cu-CF_3CO_2·2OX** (CIF)

Crystal structural file of **sql-1-Cu-CF_3CO_2·2MX** (CIF)

Crystal structural file of **sql-1-Cu-CF_3CO_2·1PX** (CIF)

■ AUTHOR INFORMATION

Corresponding Authors

Shi-Qiang Wang − *Institute of Materials Research and Engineering (IMRE), Agency for Science, Technology and Research (A*STAR), Singapore 138634, Republic of Singapore;* orcid.org/0000-0003-1213-8317; Email: wangsq@imre.a-star.edu.sg

Michael J. Zaworotko − *Bernal Institute, Department of Chemical Sciences, University of Limerick, Limerick V94 T9PX, Ireland;* orcid.org/0000-0002-1360-540X; Email: xtal@ul.ie

Authors

Catiúcia R. M. O. Matos − *Bernal Institute, Department of Chemical Sciences, University of Limerick, Limerick V94 T9PX, Ireland;* orcid.org/0000-0001-8355-396X

Shaza Darwish − *Bernal Institute, Department of Chemical Sciences, University of Limerick, Limerick V94 T9PX, Ireland;* orcid.org/0000-0001-9397-6886

Volodymyr Bon − *Department of Inorganic Chemistry I, Faculty of Chemistry and Food Chemistry, Technische Universität Dresden, Dresden 01062, Germany;* orcid.org/0000-0002-9851-5031

Yifei Luo − *Institute of Materials Research and Engineering (IMRE), Agency for Science, Technology and Research (A*STAR), Singapore 138634, Republic of Singapore;* orcid.org/0000-0002-4454-6318

Jun Zhu − *Institute of Materials Research and Engineering (IMRE), Agency for Science, Technology and Research (A*STAR), Singapore 138634, Republic of Singapore;* orcid.org/0009-0009-9735-9151

Xiaofei Zhang − *Institute of Materials Research and Engineering (IMRE), Agency for Science, Technology and Research (A*STAR), Singapore 138634, Republic of Singapore;* orcid.org/0000-0001-6292-0556

Zhengtao Xu − *Institute of Materials Research and Engineering (IMRE), Agency for Science, Technology and Research (A*STAR), Singapore 138634, Republic of Singapore;* orcid.org/0000-0002-7408-4951

Stefan Kaskel − *Department of Inorganic Chemistry I, Faculty of Chemistry and Food Chemistry, Technische Universität Dresden, Dresden 01062, Germany;* orcid.org/0000-0003-4572-0303

Complete contact information is available at: https://pubs.acs.org/10.1021/acsami.5c07908

Author Contributions

S.-Q.W.: methodology, investigation, formal analysis, writing—original draft; C.M.: investigation, writing—review and editing; S.D.: investigation, writing—review and editing; V.B.: investigation, writing—review and editing; Y.L.: investigation, writing—review and editing; J.Z.: investigation, writing—review and editing; X.Z.: investigation, writing—review and editing; Z.X.: supervision, funding acquisition; S.K.: supervision, funding acquisition, writing—review and editing; M.J.Z.: supervision, funding acquisition, writing—review and editing.

Notes

The authors declare no competing financial interest.

■ ACKNOWLEDGMENTS

M.J.Z. acknowledges the support of Research Ireland (16/IA/4624, IRCLA/2019/167). V.B. and S.K. acknowledge the German Federal Ministry of Research and Education (project nos. 05K22OD1 and 05K22OD2) for financial support. Z.X. acknowledges a startup fund from A*STAR (SC25/22-119116). Y.L. and S.-Q. W. acknowledge support from A*STAR under the Manufacturing, Trade and Connectivity (MTC) Programmatic funding scheme (M23L8b0049) and Young Individual Research Grant (M24N8c0105).

■ REFERENCES

(1) Sholl, D. S.; Lively, R. P. Seven chemical separations to change the world. *Nature* **2016**, *532* (7600), 435−437.

(2) Franz, G.; Sheldon, R. A.; *Ullmann's Encyclopedia of Industrial Chemistry*; Wiley-VCH: Weinheim, 2005.

(3) Cannella, W. J. Xylenes and Ethylbenzene. In *Kirk-Othmer Encyclopedia of Chemical Technology*; Wiley: Hoboken, 2000.

(4) Mortier, J., *Industrial Arene Chemistry: Markets, Technologies, Sustainable Processes and Cases Studies of Aromatic Commodities*; John Wiley & Sons, 2023.

(5) Yang, Y.; Bai, P.; Guo, X. Separation of Xylene Isomers: A Review of Recent Advances in Materials. *Ind. Eng. Chem. Res.* **2017**, *56* (50), 14725−14753.

(6) Lusi, M.; Barbour, L. J. Solid-Vapor Sorption of Xylenes: Prioritized Selectivity as a Means of Separating All Three Isomers Using a Single Substrate. *Angew. Chem., Int. Ed.* **2012**, *51* (16), 3928−3931.

(7) Sun, N.; Wang, S.-Q.; Zou, R.; Cui, W.-G.; Zhang, A.; Zhang, T.; Li, Q.; Zhuang, Z.-Z.; Zhang, Y.-H.; Xu, J.; Zaworotko, M. J.; Bu, X.-H. Benchmark selectivity p-xylene separation by a non-porous molecular solid through liquid or vapor extraction. *Chem. Sci.* **2019**, *10* (38), 8850−8854.

(8) Kałuża, A. M.; Mukherjee, S.; Wang, S.-Q.; O'Hearn, D. J.; Zaworotko, M. J. [Cu(4-phenylpyridine)$_4$(trifluoromethanesulfonate)$_2$], a Werner complex that exhibits high selectivity for o-xylene. *Chem. Commun.* **2020**, *56* (13), 1940−1943.

(9) du Plessis, M.; Nikolayenko, V. I.; Barbour, L. J. Record-Setting Selectivity for p-Xylene by an Intrinsically Porous Zero-Dimensional Metallocycle. *J. Am. Chem. Soc.* **2020**, *142* (10), 4529−4533.

(10) Jie, K.; Liu, M.; Zhou, Y.; Little, M. A.; Pulido, A.; Chong, S. Y.; Stephenson, A.; Hughes, A. R.; Sakakibara, F.; Ogoshi, T.; Blanc, F.; Day, G. M.; Huang, F.; Cooper, A. I. Near-Ideal Xylene Selectivity in

Adaptive Molecular Pillar[n]arene Crystals. *J. Am. Chem. Soc.* **2018**, *140* (22), 6921−6930.
(11) Moosa, B.; Alimi, L. O.; Shkurenko, A.; Fakim, A.; Bhatt, P. M.; Zhang, G.; Eddaoudi, M.; Khashab, N. M. A Polymorphic Azobenzene Cage for Energy-Efficient and Highly Selective p-Xylene Separation. *Angew. Chem., Int. Ed.* **2020**, *59* (48), 21367−21371.
(12) Rahmani, M.; Matos, C. R. M. O.; Wang, S.-Q.; Bezrukov, A. A.; Eaby, A. C.; Sensharma, D.; Hjiej-Andaloussi, Y.; Vandichel, M.; Zaworotko, M. J. Highly Selective p-Xylene Separation from Mixtures of C8 Aromatics by a Nonporous Molecular Apohost. *J. Am. Chem. Soc.* **2023**, *145* (50), 27316−27324.
(13) Zhang, G.; Zhang, K.; Lou, X. Y.; Li, X.; Song, C. L.; Huan, W. W.; Yang, Y. W. Separation of p-Xylene from C8 Alkylaromatics by Nonporous Adaptive Crystals of Leggero Pillar[4]arene[1]quinone. *ACS Mater. Lett.* **2024**, *6* (2), 446−451.
(14) Alaerts, L.; Kirshhock, C. E. A.; Maes, M.; van der Veen, M. A.; Finsy, V.; Depla, A.; Martens, J. A.; Baron, G. V.; Jacobs, P. A.; Denayer, J. F. M.; De Vos, D. E. Selective adsorption and separation of xylene isomers and ethylbenzene with the microporous vanadium-(IV) terephthalate MIL-47. *Angew. Chem., Int. Ed.* **2007**, *46* (23), 4293−4297.
(15) Alaerts, L.; Maes, M.; Giebeler, L.; Jacobs, P. A.; Martens, J. A.; Denayer, J. F. M.; Kirschhock, C. E. A.; De Vos, D. E. Selective Adsorption and Separation of ortho-Substituted Alkylaromatics with the Microporous Aluminum Terephthalate MIL-53. *J. Am. Chem. Soc.* **2008**, *130* (43), 14170−14178.
(16) Vermoortele, F.; Maes, M.; Moghadam, P. Z.; Lennox, M. J.; Ragon, F.; Boulhout, M.; Biswas, S.; Laurier, K. G. M.; Beurroies, I.; Deboyel, R.; Roeffaers, M.; Stock, N.; Duren, T.; Serre, C.; De Vos, D. E. E., p-Xylene-Selective Metal-Organic Frameworks: A Case of Topology-Directed Selectivity. *J. Am. Chem. Soc.* **2011**, *133* (46), 18526−18529.
(17) Warren, J. E.; Perkins, G. C.; Jelfs, K. E.; Boldrin, P.; Chater, P. A.; Miller, G. J.; Manning, T. D.; Briggs, M. E.; Stylianou, K. C.; Claridge, J. B.; Rosseinsky, M. J. Shape Selectivity by Guest-Driven Restructuring of a Porous Material. *Angew. Chem., Int. Ed.* **2014**, *53* (18), 4592−4596.
(18) Torres-Knoop, A.; Krishna, R.; Dubbeldam, D. Separating Xylene Isomers by Commensurate Stacking of p-Xylene within Channels of MAF-X8. *Angew. Chem., Int. Ed.* **2014**, *53* (30), 7774−7778.
(19) Gonzalez, M. I.; Kapelewski, M. T.; Bloch, E. D.; Milner, P. J.; Reed, D. A.; Hudson, M. R.; Mason, J. A.; Barin, G.; Brown, C. M.; Long, J. R. Separation of Xylene Isomers through Multiple Metal Site Interactions in Metal-Organic Frameworks. *J. Am. Chem. Soc.* **2018**, *140* (9), 3412−3422.
(20) Yang, X.; Zhou, H.-L.; He, C.-T.; Mo, Z.-W.; Ye, J.-W.; Chen, X.-M.; Zhang, J.-P. Flexibility of Metal-Organic Framework Tunable by Crystal Size at the Micrometer to Submillimeter Scale for Efficient Xylene Isomer Separation. *Research* **2019**, *2019*, 9463719.
(21) Kim, S.-I.; Lee, S.; Chung, Y. G.; Bae, Y.-S. Origin of p-xylene selectivity in a DABCO pillar-layered metal-organic framework: Combined experimental and computational investigation. *ACS Appl. Mater. Interfaces* **2019**, *11* (34), 31227−31236.
(22) Cui, X.; Niu, Z.; Shan, C.; Yang, L.; Hu, J.; Wang, Q.; Lan, P. C.; Li, Y.; Wojtas, L.; Ma, S.; Xing, H. Efficient separation of xylene isomers by a guest-responsive metal−organic framework with rotational anionic sites. *Nat. Commun.* **2020**, *11* (1), 5456.
(23) Li, X.; Wang, J.; Bai, N.; Zhang, X.; Han, X.; da Silva, I.; Morris, C. G.; Xu, S.; Wilary, D. M.; Sun, Y.; Cheng, Y.; Murray, C. A.; Tang, C. C.; Frogley, M. D.; Cinque, G.; Lowe, T.; Zhang, H.; Ramirez-Cuesta, A. J.; Thomas, K. M.; Bolton, L. W.; Yang, S.; Schröder, M. Refinement of pore size at sub-angstrom precision in robust metal−organic frameworks for separation of xylenes. *Nat. Commun.* **2020**, *11* (1), 4280.
(24) Polyukhov, D. M.; Poryvaev, A. S.; Sukhikh, A. S.; Gromilov, S. A.; Fedin, M. V. Fine-Tuning Window Apertures in ZIF-8/67 Frameworks by Metal Ions and Temperature for High-Efficiency Molecular Sieving of Xylenes. *ACS Appl. Mater. Interfaces* **2021**, *13* (34), 40830−40836.
(25) Idrees, K. B.; Li, Z.; Xie, H.; Kirlikovali, K. O.; Kazem-Rostami, M.; Wang, X.; Wang, X.; Tai, T.-Y.; Islamoglu, T.; Stoddart, J. F.; Snurr, R. Q.; Farha, O. K. Separation of Aromatic Hydrocarbons in Porous Materials. *J. Am. Chem. Soc.* **2022**, *144* (27), 12212−12218.
(26) Li, L.; Guo, L.; Olson, D. H.; Xian, S.; Zhang, Z.; Yang, Q.; Wu, K.; Yang, Y.; Bao, Z.; Ren, Q.; Li, J. Discrimination of xylene isomers in a stacked coordination polymer. *Science* **2022**, *377* (6603), 335−339.
(27) Ye, Z.-M.; Zhang, X.-F.; Liu, D.-X.; Xu, Y.-T.; Wang, C.; Zheng, K.; Zhou, D.-D.; He, C.-T.; Zhang, J.-P. A gating ultramicroporous metal-organic framework showing high adsorption selectivity, capacity and rate for xylene separation. *Sci. China: Chem.* **2022**, *65* (8), 1552−1558.
(28) Gao, M.-Y.; Wang, S.-Q.; Bezrukov, A. A.; Darwish, S.; Song, B.-Q.; Deng, C.; Matos, C. R. M. O.; Liu, L.; Tang, B.; Dai, S.; Yang, S.; Zaworotko, M. J. Switching Adsorbent Layered Material that Enables Stepwise Capture of C8 Aromatics via Single-Crystal-to-Single-Crystal Transformations. *Chem. Mater.* **2023**, *35* (23), 10001−10008.
(29) Yu, L.; Zhang, J.; Ullah, S.; Yao, J.; Luo, H.; Huang, J.; Xia, Q.; Thonhauser, T.; Li, J.; Wang, H. Separating Xylene Isomers with a Calcium Metal-Organic Framework. *Angew. Chem., Int. Ed.* **2023**, *62* (41), No. e202310672.
(30) Wang, Q.; Li, Y.; Qiu, Z.; Zhou, D.; Yang, L.; Suo, X.; Cui, X.; Xing, H. Highly Efficient Separation of Intermediate-Size m-Xylene from Xylenes via a Length-Matched Metal-Organic Framework with Optimal Oxygen Sites Distribution. *Angew. Chem., Int. Ed.* **2024**, *63* (46), No. e202408817.
(31) Hyun, T.; Park, J.; So, J.; Kim, J.; Koh, D.-Y. Unexpected Molecular Sieving of Xylene Isomer Using Tethered Ligand in Polymer-Metal-Organic Frameworks (polyMOFs). *Adv. Sci.* **2024**, *11* (34), 2402980.
(32) Xie, X.-J.; Zeng, H.; Huang, Y.-L.; Wang, Y.; Cao, Q.-Y.; Lu, W.; Li, D. Direct production of o-xylene from six-component BTEXs using a channel-pore interconnected metal-organic framework. *Chem* **2025**, *11*, 102339.
(33) Perry, J. J., IV; Perman, J. A.; Zaworotko, M. J. Design and synthesis of metal−organic frameworks using metal−organic polyhedra as supermolecular building blocks. *Chem. Soc. Rev.* **2009**, *38* (5), 1400−1417.
(34) Cook, T. R.; Zheng, Y.-R.; Stang, P. J. Metal-Organic Frameworks and Self-Assembled Supramolecular Coordination Complexes: Comparing and Contrasting the Design, Synthesis, and Functionality of Metal-Organic Materials. *Chem. Rev.* **2013**, *113* (1), 734−777.
(35) Moulton, B.; Zaworotko, M. J. From Molecules to Crystal Engineering: Supramolecular Isomerism and Polymorphism in Network Solids. *Chem. Rev.* **2001**, *101*, 1629−1658.
(36) Yaghi, O. M.; O'Keeffe, M.; Ockwig, N. W.; Chae, H. K.; Eddaoudi, M.; Kim, J. Reticular synthesis and the design of new materials. *Nature* **2003**, *423* (6941), 705−714.
(37) Wu, H.; Gong, Q.; Olson, D. H.; Li, J. Commensurate Adsorption of Hydrocarbons and Alcohols in Microporous Metal Organic Frameworks. *Chem. Rev.* **2012**, *112* (2), 836−868.
(38) Van de Voorde, B.; Bueken, B.; Denayer, J.; De Vos, D. Adsorptive separation on metal−organic frameworks in the liquid phase. *Chem. Soc. Rev.* **2014**, *43* (16), 5766−5788.
(39) Bao, Z.; Chang, G.; Xing, H.; Krishna, R.; Ren, Q.; Chen, B. Potential of microporous metal-organic frameworks for separation of hydrocarbon mixtures. *Energy Environ. Sci.* **2016**, *9* (12), 3612−3641.
(40) Zhang, Z.; Peh, S. B.; Kang, C.; Chai, K.; Zhao, D. Metal-organic frameworks for C6−C8 hydrocarbon separations. *EnergyChem* **2021**, *3* (4), 100057.
(41) Liu, Y.; Wang, C.; Yang, Q.; Ren, Q.; Bao, Z. Separation of xylene isomers using metal-organic frameworks: Addressing challenges in the petrochemical industry. *Coord. Chem. Rev.* **2025**, *523*, 216229.

https://doi.org/10.1021/acsami.5c07908
ACS Appl. Mater. Interfaces XXXX, XXX, XXX−XXX

(42) Xu, M.; Tang, W.-Q.; Meng, S.-S.; Gu, Z.-Y. Metal−organic frameworks for the separation of xylene isomers. *Chem. Soc. Rev.* **2025**, *54* (3), 1613−1633.
(43) Horike, S.; Shimomura, S.; Kitagawa, S. Soft porous crystals. *Nat. Chem.* **2009**, *1* (9), 695−704.
(44) Schneemann, A.; Bon, V.; Schwedler, I.; Senkovska, I.; Kaskel, S.; Fischer, R. A. Flexible metal-organic frameworks. *Chem. Soc. Rev.* **2014**, *43* (16), 6062−6096.
(45) Chang, Z.; Yang, D.-H.; Xu, J.; Hu, T.-L.; Bu, X.-H. Flexible Metal-Organic Frameworks: Recent Advances and Potential Applications. *Adv. Mater.* **2015**, *27* (36), 5432−5441.
(46) Zhang, J.-P.; Zhou, H.-L.; Zhou, D.-D.; Liao, P.-Q.; Chen, X.-M. Controlling flexibility of metal−organic frameworks. *Natl. Sci. Rev.* **2018**, *5* (6), 907−919.
(47) Krause, S.; Hosono, N.; Kitagawa, S. Chemistry of Soft Porous Crystals: Structural Dynamics and Gas Adsorption Properties. *Angew. Chem., Int. Ed.* **2020**, *59* (36), 15325−15341.
(48) Wang, S.-Q.; Mukherjee, S.; Zaworotko, M. J. Spiers Memorial Lecture: Coordination Networks that Switch between Nonporous and Porous Structures: An Emerging Class of Soft Porous Crystals. *Faraday Discuss* **2021**, *231*, 9−50.
(49) Senkovska, I.; Bon, V.; Abylgazina, L.; Mendt, M.; Berger, J.; Kieslich, G.; Petkov, P.; Luiz Fiorio, J.; Joswig, J.-O.; Heine, T.; Schaper, L.; Bachetzky, C.; Schmid, R.; Fischer, R. A.; Pöppl, A.; Brunner, E.; Kaskel, S. Understanding MOF Flexibility: An Analysis Focused on Pillared Layer MOFs as a Model System. *Angew. Chem., Int. Ed.* **2023**, *62* (33), No. e202218076.
(50) Zhang, J.-P.; Liao, P.-Q.; Zhou, H.-L.; Lin, R.-B.; Chen, X.-M. Single-crystal X-ray diffraction studies on structural transformations of porous coordination polymers. *Chem. Soc. Rev.* **2014**, *43* (16), 5789−5814.
(51) Bon, V.; Brunner, E.; Pöppl, A.; Kaskel, S. Unraveling Structure and Dynamics in Porous Frameworks via Advanced In Situ Characterization Techniques. *Adv. Funct. Mater.* **2020**, *30* (41), 1907847.
(52) Wang, S.-Q.; Yang, Q.-Y.; Mukherjee, S.; O'Nolan, D.; Patyk-Kazmierczak, E.; Chen, K.-J.; Shivanna, M.; Murray, C.; Tang, C. C.; Zaworotko, M. J. Recyclable switching between nonporous and porous phases of a square lattice (sql) topology coordination network. *Chem. Commun.* **2018**, *54* (51), 7042−7045.
(53) Wang, S.-Q.; Mukherjee, S.; Patyk-Kaźmierczak, E.; Darwish, S.; Bajpai, A.; Yang, Q.-Y.; Zaworotko, M. J. Highly Selective, High-Capacity Separation of o-Xylene from C8 Aromatics by a Switching Adsorbent Layered Material. *Angew. Chem., Int. Ed.* **2019**, *58* (20), 6630−6634.
(54) Wang, S.-Q.; Darwish, S.; Sensharma, D.; Zaworotko, M. J. Tuning the switching pressure in square lattice coordination networks by metal cation substitution. *Mater. Adv.* **2022**, *3* (2), 1240−1247.
(55) Wang, S.-Q.; Darwish, S.; Meng, X.-Q.; Chang, Z.; Bu, X.-H.; Zaworotko, M. J. Acetylene storage performance of $[Ni(4,4'\text{-bipyridine})_2(NCS)_2]_n$, a switching square lattice coordination network. *Chem. Commun.* **2022**, *58* (10), 1534−1537.
(56) Wang, S.-Q.; Darwish, S.; Zaworotko, M. J. Adsorbate-dependent phase switching in the square lattice topology coordination network $[Ni(4,4'\text{-bipyridine})_2(NCS)_2]_n$. *Chem. Commun.* **2023**, *59* (5), 559−562.
(57) Wang, S.-Q.; Bon, V.; Darwish, S.; Wang, S.-M.; Yang, Q.-Y.; Xu, Z.; Kaskel, S.; Zaworotko, M. J. Insight into the Gas-Induced Phase Transformations in a 2D Switching Coordination Network via Coincident Gas Sorption and In Situ PXRD. *ACS Mater. Lett.* **2024**, *6* (2), 666−673.
(58) Kumar, N.; Wang, S.-Q.; Mukherjee, S.; Bezrukov, A. A.; Patyk-Kaźmierczak, E.; O'Nolan, D.; Kumar, A.; Yu, M.-H.; Chang, Z.; Bu, X.-H.; Zaworotko, M. J. Crystal engineering of a rectangular sql coordination network to enable xylenes selectivity over ethylbenzene. *Chem. Sci.* **2020**, *11* (26), 6889−6895.
(59) Gu, Z.-Y.; Jiang, D.-Q.; Wang, H.-F.; Cui, X.-Y.; Yan, X.-P. Adsorption and separation of xylene isomers and ethylbenzene on two Zn-terephthalate metal-organic frameworks. *J. Phys. Chem. C* **2010**, *114* (1), 311−316.
(60) Van der Perre, S.; Van Assche, T.; Bozbiyik, B.; Lannoeye, J.; De Vos, D. E.; Baron, G. V.; Denayer, J. F. M. Adsorptive Characterization of the ZIF-68 Metal-Organic Framework: A Complex Structure with Amphiphilic Properties. *Langmuir* **2014**, *30* (28), 8416−8424.
(61) Lannoeye, J.; Van de Voorde, B.; Bozbiyik, B.; Reinsch, H.; Denayer, J.; De Vos, D. An aliphatic copper metal-organic framework as versatile shape selective adsorbent in liquid phase separations. *Microporous Mesoporous Mater.* **2016**, *226*, 292−298.
(62) Gee, J. A.; Zhang, K.; Bhattacharyya, S.; Bentley, J.; Rungta, M.; Abichandani, J. S.; Sholl, D. S.; Nair, S. Computational Identification and Experimental Evaluation of Metal-Organic Frameworks for Xylene Enrichment. *J. Phys. Chem. C* **2016**, *120* (22), 12075−12082.
(63) Shivanna, M.; Otake, K.-I.; Zheng, J.-J.; Sakaki, S.; Kitagawa, S. Control of local flexibility towards p-xylene sieving in Hofmann-type porous coordination polymers. *Chem. Commun.* **2020**, *56* (67), 9632−9635.
(64) Sapianik, A. A.; Dudko, E. R.; Kovalenko, K. A.; Barsukova, M. O.; Samsonenko, D. G.; Dybtsev, D. N.; Fedin, V. P. Metal-Organic Frameworks for Highly Selective Separation of Xylene Isomers and Single-Crystal X-ray Study of Aromatic Guest-Host Inclusion Compounds. *ACS Appl. Mater. Interfaces* **2021**, *13* (12), 14768−14777.
(65) Lin, Y.; Zhang, J.; Pandey, H.; Dong, X.; Gong, Q.; Wang, H.; Yu, L.; Zhou, K.; Yu, W.; Huang, X.; Thonhauser, T.; Han, Y.; Li, J. Efficient separation of xylene isomers by using a robust calcium-based metal−organic framework through a synergetic thermodynamically and kinetically controlled mechanism. *J. Mater.Chem. A* **2021**, *9* (46), 26202−26207.
(66) Ye, J.; du Plessis, M.; Loots, L.; van Wyk, L. M.; Barbour, L. J. Solid−Liquid Separation of Xylene Isomers Using a Cu-Based Metallocycle. *Cryst. Growth Des.* **2022**, *22* (4), 2654−2661.
(67) Chen, K.; Liu, P.; Wang, Y.; Ren, Y.; Li, J.; Chen, Y.; Li, J.; Li, L. Structural functionalization in robust metal−organic frameworks for p-xylene separation with superior adsorption capacity. *Microporous Mesoporous Mater.* **2023**, *360*, 112705.
(68) Deng, X.; Deng, M.; Li, Y.-L.; Liu, Z.; Liu, T.-F.; Chen, X.; Cai, S.; Liu, B.; Li, J.; Lv, D.; Li, J.; Yuan, W. A zinc-octacarboxylate MOF with an unusual (6, 8)-connected ocu topology for high-capacity adsorptive separation of C8 alkylaromatics. *Chem. Eng. J.* **2023**, *474*, 145694.
(69) Bae, H. J.; Kim, S.-I.; Choi, Y.; Kim, K.-M.; Bae, Y.-S. High p-xylene selectivity in aluminum-based metal−organic framework with 1-D channels. *J. Ind. Eng. Chem.* **2023**, *117*, 333−341.
(70) Yang, L.; Liu, H.; Yuan, D.; Xing, J.; Xu, Y.; Liu, Z. Efficient Separation of Xylene Isomers by a Pillar-Layer Metal−Organic Framework. *ACS Appl. Mater. Interfaces* **2021**, *13* (35), 41600−41608.

https://doi.org/10.1021/acsami.5c07908
ACS Appl. Mater. Interfaces XXXX, XXX, XXX−XXX